GEOPHYSICAL RESEARCH LETTERS, VOL. 37, L09102, doi:10.1029/2010GL042980, 2010

Electron beams as the source of whistler-mode auroral hiss at Saturn

A. J. Kopf,[1] D. A. Gurnett,[1] J. D. Menietti,[1] P. Schippers,[1] C. S. Arridge,[2,3] G. B. Hospodarsky,[1] W. S. Kurth,[1] S. Grimald,[4] N. André,[4] A. J. Coates,[2,3] and M. K. Dougherty[5]

Received 23 February 2010; revised 26 March 2010; accepted 30 March 2010; published 4 May 2010.

[1] Over the last three years, the Cassini spacecraft has been in a series of high inclination orbits, allowing investigation and measurements of Saturnian auroral phenomena. During this time, the Radio and Plasma Wave Science (RPWS) Investigation on Cassini detected low frequency whistler mode emissions propagating upward along the auroral field lines, much like terrestrial auroral hiss. Comparisons of RPWS data with Cassini Plasma Spectrometer (CAPS) plasma measurements during a high-latitude pass on 17 October 2008, show that intense upward moving electron beams with energies of a few hundred eV were associated with auroral hiss emissions. In this paper we show that these beams produce large growth rates for whistler-mode waves propagating along the resonance cone, similar to the generation of auroral hiss at Earth. **Citation:** Kopf, A. J., et al. (2010), Electron beams as the source of whistler-mode auroral hiss at Saturn, *Geophys. Res. Lett.*, *37*, L09102, doi:10.1029/2010GL042980.

1. Introduction

[2] Auroral hiss is a whistler-mode plasma wave emission found in high-latitude regions of planetary magnetospheres. This emission was first discovered at Earth using ground based instruments [*Martin et al.*, 1960], and later studied by satellites [*Gurnett and O'Brien*, 1964; *Gurnett*, 1966]. Similar emissions have also been detected at Jupiter [*Gurnett et al.*, 1979; *Farrell et al.*, 1993; *Gurnett et al.*, 2005] and Saturn [*Gurnett et al.*, 2009]. Auroral hiss is known to propagate in the whistler mode at frequencies beneath both the electron cyclotron frequency and electron plasma frequency. On a frequency-time spectrogram, this emission displays a funnel shape with a V-shaped low-frequency cutoff, explained by emission from a localized source propagating near the resonance cone [*Smith*, 1969; *Mosier and Gurnett*, 1969; *James*, 1976].

[3] Auroral hiss originates from the high-latitude regions of planetary magnetospheres, and is known to be produced by electron beams associated with the aurora. Initially auroral hiss was believed to be produced by incoherent Cherenkov radiation [*Jørgensen*, 1968]. However, this theory later proved insufficient to explain the observed intensities, which were far too large for this mechanism [*Taylor and Shawhan*, 1974]. Around the same time, sounding rocket experiments observed whistler mode plasma waves in conjunction with an artificially injected electron beam [*Cartwright and Kellogg*, 1974; *Monson et al.*, 1976]. *Maggs* [1976] first suggested that auroral hiss was generated by a coherent beam-plasma interaction at the Landau resonance velocity. An artificial beam experiment aboard the Space Shuttle later confirmed this theory [*Gurnett et al.*, 1986; *Farrell et al.*, 1989].

[4] Recently, strong evidence that field-aligned electron beams generate terrestrial auroral hiss has been obtained by the Fast Auroral SnapshoT Explorer (FAST) [*Pfaff et al.*, 2001]. The FAST satellite carries a high-resolution plasma instrument, and has shown that roughly 85% of auroral hiss emissions are generated by intense, low-energy, upward-propagating electrons in the downward current region of the aurora [*Ergun et al.*, 2003]. In this paper, we will show examples of the same relationship at Saturn, and will calculate the whistler-mode growth rates of upward propagating electron beams to demonstrate their ability to produce the observed auroral hiss intensities.

2. Observations

[5] The Saturn-orbiting Cassini spacecraft carries the Radio and Plasma Wave Science (RPWS) Investigation, which is capable of detecting a wide range of radio and plasma wave emissions. The RPWS instrument makes measurements of wave electric and magnetic fields, and can also determine the electron density and temperature via a Langmuir Probe [*Gurnett et al.*, 2004]. In addition, Cassini carries the Cassini Plasma Spectrometer (CAPS), which measures the flux of ions and electrons as a function of energy per charge and viewing direction [*Young et al.*, 2004]. When combined with data from the Cassini Magnetometer (MAG), this information can be used to compute distributions in terms of energy and pitch angle. The component of CAPS that measures electrons is called the Electron Spectrometer (ELS).

[6] On 17 October 2008, the Cassini spacecraft was in a high-latitude pass at very low altitudes. During this pass, at 8:35 UT, ELS detected an intense, upward-propagating, field-aligned electron beam at an energy of about 200 eV, shown in Figure 1. The beam can be seen in Figure 1 as the enhancement in the phase-space density along the negative

[1]Department of Physics and Astronomy, University of Iowa, Iowa City, Iowa, USA.
[2]Mullard Space Science Laboratory, University College London, Dorking, U.K.
[3]Centre for Planetary Sciences, UCL-Birkbeck, London, U.K.
[4]Centre d'Etude Spatiale des Rayonnements, Université Paul Sabatier, CNRS, Toulouse, France.
[5]Blackett Laboratory, Imperial College, London, U.K.

0094-8276/10/2010GL042980

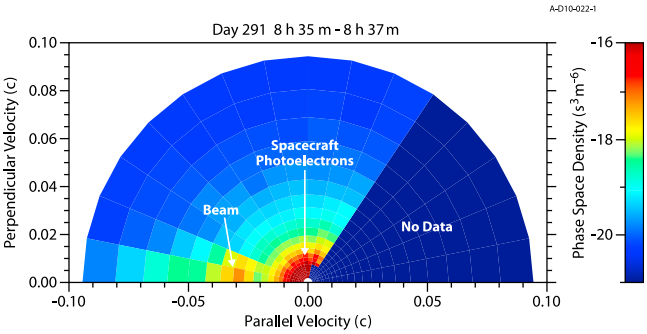

Figure 1. An ELS pitch-angle distribution from the 17 October 2008 event, plotted as a function of parallel and perpendicular velocities, and color coded for phase space density. The data were collected over a two-minute interval to provide good pitch angle coverage. An electron beam appears as an enhancement in the density in the lower left near the horizontal axis, at a velocity corresponding to about 200 eV.

horizontal axis. The ELS data in Figure 1 have been integrated over two minutes to provide good pitch-angle coverage. This upward propagating electron beam is exactly the type of velocity distribution expected for the generation of auroral hiss via a beam-plasma instability [*Maggs*, 1976].

[7] At the same time as the beam, strong broadband low-frequency emissions, likely in the whistler-mode, were also observed by RPWS, as shown in Figure 2. This emission does not display the typical funnel-shaped emission of auroral hiss, instead appearing more burst-like in nature. However, this is not unlike terrestrial auroral hiss, which often displays similar burst-like electrostatic noise in the source region [*Lönnqvist et al.*, 1993]. Wave magnetic field measurements were too weak to allow a determination of the direction of propagation, although a nearby V-shaped auroral hiss feature at roughly 11:30 UT has been confirmed to be upward-propagating.

3. Whistler-mode Growth Rates

[8] In order to show that this electron beam can be the source of the simultaneously occurring whistler-mode radiation, the resulting plasma dispersion relation must be analyzed to obtain the growth rate. Similar calculations have been performed at Earth by *Maggs* [1976], but we present here the first such results at Saturn.

3.1. Analytical Analysis

[9] To calculate the growth rate analytically, we follow the model used by *Morgan et al.* [1994]. The starting point comes from *Kennel* [1966], who derived the linear growth rate for waves propagating in a collisionless, homogeneous, magnetized plasma, assuming resonance velocities well above the thermal velocity of the distribution function, and a growth rate that is small compared to the wave frequency. His formula is lengthy and therefore is not repeated here. However, a few simple assumptions reduce it to a more manageable form. First, we assume that the waves are propagating near the resonance cone, which is expected for auroral hiss [*Mosier and Gurnett*, 1969]. Second, we assume that ions play a negligible role in the wave propagation. Kennel's equation then reduces to

$$\gamma \frac{\partial D^{(0)}}{\partial \omega} = \frac{8\pi^2 n^4 \omega_p^2}{k^2 n_0 |\cos(\theta)|} \sum_m \int_0^\infty dv_\perp J_m^2 \left(\frac{k_\perp v_\perp}{\omega_c}\right) \cdot \left[\frac{m\omega_c}{k}\frac{\partial f}{\partial v_\perp} + v_\perp \cos(\theta)\frac{\partial f}{\partial v_{||}}\right] \quad (1)$$

where γ is the growth rate, $D^{(0)}$ is the cold plasma determinant defined by *Stix* [1962], n is the index of refraction, ω_p is the plasma frequency, k is the wave number, n_0 is the electron density, θ is the wave normal angle, ω_c is the electron cyclotron frequency, f is the phase-space distribution function, and J_m is a Bessel function of order m. The parallel component of the velocity, $v_{||}$, is evaluated at the resonance velocity, $\omega/k_{||}$.

[10] From Figure 2, we observe that at 8:35 UT, the electron cyclotron frequency, ω_c, as calculated from magnetometer measurements, is on the order of 10 kHz. Measurements of the electron density from the Langmuir Probe and the CAPS instrument show that the electron plasma frequency, ω_p, is much lower, roughly 500 Hz. As a result, we now make the approximation that $\omega_c^2 \gg \omega_p^2 > \omega^2$. While this condition is not true for all times at Saturn, it holds in the cases presented in this paper, and greatly simplifies Equation (1). We further recognize that we only need the m = 0 term in the Bessel Function series. For the observed beam velocities, it is easy to show that the wavelength of the whistler mode is much longer than the cyclotron radius. As a result, the terms where m is nonzero become negligible compared to the m = 0 term when convolved with the observed distribution function. This eliminates the first term of the integral, leaving only the $\partial f/\partial v_{||}$ term. Also, since the

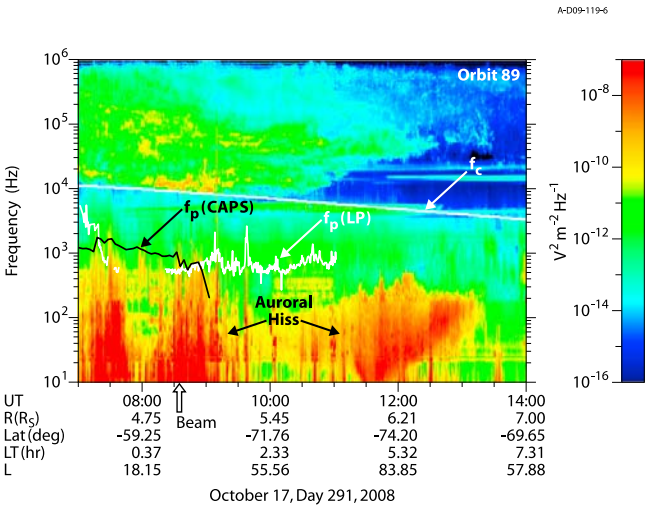

Figure 2. Seven hours of RPWS data from 17 October 2008. An auroral hiss funnel appears near 11:30 UT, along with burst-like low-frequency emission at earlier times. The white line labeled f_c indicates the electron cyclotron frequency. The white line labeled f_p (LP) is the electron plasma frequency from the Langmuir probe, and the black line labeled f_p (CAPS) is the electron plasma frequency from the CAPS plasma instruments. The intense beam detected at 8:35 UT is marked along the horizontal axis.

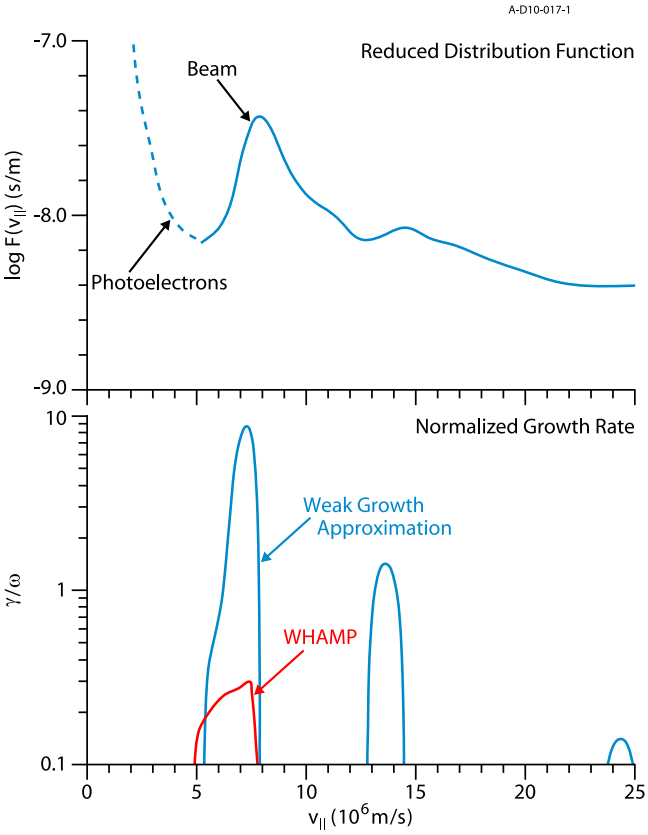

Figure 3. The reduced distribution and growth rate for the 8:35 UT beam on 17 October 2008. (top) A region of large positive slope, shown in blue, which yields (bottom) the growth. The two regions of significant growth result from two bumps in the distribution function, indicating the beam includes multiple components. The analytical result indicates a very large growth rate, too large for the weak growth approximation to be valid. The WHAMP numerical result (shown in red) does not rely on the weak growth approximation and still shows a very high growth rate, $\gamma/\omega \approx 0.3$.

argument of the Bessel function can be shown to be small, we can approximate J_0^2 as 1. Cancelling common terms yields

$$\gamma = \frac{2\pi\omega_p^2\omega}{k^2}\frac{\partial}{\partial v_\parallel}\frac{1}{n_0}\int_0^\infty dv_\perp 2\pi v_\perp f(v_\perp, v_\parallel). \quad (2)$$

Finally, we define the reduced distribution function as

$$F(v_\parallel) = \frac{1}{n_0}\int_0^\infty dv_\perp 2\pi v_\perp f(v_\perp, v_\parallel). \quad (3)$$

Inserting this into Equation (2), along with the Landau resonance condition for the wave number, produces the following equation for the growth rate

$$\gamma = \frac{2\pi\omega_p^2 v_\parallel^2 \cos^2(\theta_{res})}{\omega}\frac{\partial F}{\partial v_\parallel}, \quad (4)$$

where θ_{res} is the resonance cone angle, which is determined by the values of the cyclotron and plasma frequencies [*Mosier and Gurnett*, 1969].

[11] Our approach to evaluating the growth rate is to perform an interpolation of the measured plasma distribution function, smooth it into a continuous mesh, and then approximate the integration with a summation over the discrete points. Due to the close proximity that most of the data points have to each other, which limits the variation in the values of the distribution between points, a simple bilinear approximation method was utilized to create the smooth mesh. This smoothing took the roughly 300 ELS data points, which were oriented in a polar grid in velocity space, and transformed them into a linear grid containing well over 3000 points, making it easy to perform the necessary summations with good accuracy to obtain the reduced distribution function.

[12] The first case we examine is the beam shown earlier, at or around 8:35 UT, in the region of burst-like low-frequency emission in Figure 2. Figure 3 displays the results of the analytical calculation of the growth rate at a representative frequency of 100 Hz for this time period. The values of the electron cyclotron and plasma frequencies listed earlier, $\omega_c \approx 10$ kHz and $\omega_p \approx 500$ Hz, were used in this calculation. The top panel is the reduced distribution function calculated from the bilinear interpolation and integration of the ELS data. The dashed region marks the photoelectrons generated by the spacecraft, which are not part of the Saturn environment but cannot be easily removed from the interpolated results. The beam appears after the photoelectrons, where an enhancement in the distribution forms a bump-on-tail distribution. The lower panel displays the calculated growth rates. Two significant regions of growth appear in the growth calculation, resulting from the two regions of positive slope in the distribution. This indicates that the beam, while dominated by 200 eV electrons, has multiple components. The resulting normalized growth rate, γ/ω, is very large, significantly greater than one. Such a large growth rate indicates a very rapidly growing instability, but violates the weak-growth approximation inherent in Kennel's equation, suggesting that another approach must be used to obtain an accurate growth rate.

3.2. Numerical Analysis

[13] Since the analytical analysis did not give accurate results, it is necessary to perform numerical calculations using a technique that does not rely on the weak-growth approximation. Among the techniques that can be used is a computer program known as WHAMP (Waves in Homogeneous Anisotropic Multicomponent Plasmas), which was developed by *Rönnmark* [1982, 1983] and designed to solve the dispersion relation for waves in a magnetized plasma for which the distribution function can be described as a sum of Maxwellian velocity distributions. The program allows for up to six Maxwellian components, and yields a solution to the dispersion relation, as well as values for the growth rate and group velocity.

[14] In the case of the 8:35 UT beam, after subtracting out the spacecraft photoelectrons, two bi-Maxwellian components were used to fit the distribution, in order to provide dimension in both the parallel and perpendicular directions with respect to the magnetic field. These two components were fit to the two bumps in the distribution, which can be

observed in the top panel of Figure 3 at roughly 7×10^6 m/s and 14×10^6 m/s. In both cases, some of the input parameters, such as the density and temperature, could be determined from the RPWS and ELS instruments, while the other input parameters were adjusted to provide a good fit to the ELS measurement.

[15] In addition to the analytical results, the lower panel of Figure 3 also displays the numerical growth rates from the WHAMP calculation. These growth rates are significantly smaller than the analytical results, since WHAMP provides a full solution to the dispersion relation without assuming weak growth. However, the growth rates are still quite large, $\gamma/\omega \approx 0.3$, confirming that this beam is capable of producing the observed radio emission, as suggested by the analytical result. In fact, since the wave energy after a time t is proportional to $e^{2\gamma t}$, the growth of this wave energy over just one second would be approximately e^{377} for a characteristic frequency of 100 Hz, large enough to be significant for even the smallest conceivable background intensities in the amplifying region.

[16] The 8:35 UT beam is not the only such event during this orbit. In analyzing all two-minute intervals from 7:00–9:30 UT, seven other intervals were found to contain beams at similar energies, though all of these beams were considerably weaker in intensity. Analysis of these events using Equation (4) yielded growth rates of $\gamma/\omega \approx 0.3$ in the largest cases, in the range of the WHAMP result from the 8:35 UT calculation, though some were more than an order of magnitude smaller. As a result, all of these were deemed small enough that numerical calculation was not required. All of these beams coincided with regions of auroral hiss emission.

4. Discussion

[17] In this paper, we have presented the analysis of a series of electron beams detected during the Cassini spacecraft's high-latitude pass on 17 October 2008. In each case, not only did the detected beam coincide with auroral hiss emission, but growth rate analyses demonstrated that each beam possessed large whistler-mode growth rates, sufficient to produce the observed emission intensities. In the case of the 8:35 UT beam, these growth rates were even so large as to violate the weak growth approximation.

[18] Compared to auroral hiss typically observed at Earth, the emission observed during the period analyzed possesses two notable characteristics. First, the emission is burst-like, with numerous variations on short time scales. In addition, in some regions, the emission extends to frequencies above the local plasma frequency, which is not possible for the whistler mode.

[19] Instead of possessing a smooth upper boundary, the emission around 8:35 UT contains burst-like temporal variations on the order of the instrument's temporal resolution. These bursts appear in Figure 2 as fine structure at the higher frequencies of the auroral hiss emission. We considered the possibility that this pattern could be indicative of solitary wave structures, but inspection of the waveforms has not revealed the presence of any such waves. Analysis of high-resolution ELS data has revealed extremely large fluctuations in the beam intensity on time scales on the order of the ELS instrument resolution, two seconds. With this in mind, it is not surprising to see short term temporal variations in the intensity of the auroral hiss, as variations in the beam intensity would produce variable growth rates. Furthermore, this region may contain emission due to ion conics, as reported by *Mitchell et al.* [2009], which are commonly observed at Saturn. This emission is also burst-like, and would enhance the intensity observed by RPWS.

[20] The final notable aspect of the emission is the occasional extension to frequencies above the local electron plasma frequency. Many of these extensions are observed around the time of the 8:35 UT beam. Since the whistler mode is restricted to frequencies below the lesser of the electron cyclotron frequency and electron plasma frequency, such an upward extension is not possible. However, because whistler-mode waves are driven into resonance as they approach the $f = f_p$ surface, the wave vector, k, becomes very large. At resonance, the corresponding wavelength becomes very small, and Doppler effects caused by spacecraft and plasma motions can become significant. These effects can push the observed emission to higher frequencies than are present in the plasma rest frame, which would explain why the observed frequency occasionally extends above the plasma frequency.

[21] **Acknowledgments.** The research at the University of Iowa was supported by NASA through contract 1356500 with the Jet Propulsion Laboratory. C.S.A., A.J.C. and S.G. were supported by the Science and Technology Facilities Council (STFC) Rolling grant to MSSL/UCL. C.S.A. was supported by a Science and Technology Facilities Council (STFC) Postdoctoral fellowship. CAPS-ELS operations were supported in the UK by STFC and C.S.A. thanks G.R. Lewis and N. Shane for data reduction and software support.

References

Cartwright, D. G., and P. J. Kellogg (1974), Observations of radiation from an electron beam artificially injected into the ionosphere, *J. Geophys. Res.*, *79*, 1439–1457, doi:10.1029/JA079i010p01439.

Ergun, R. E., et al. (2003), Fast auroral snapshot satellite observations of very low frequency saucers, *Phys. Plasmas*, *10*(2), 454–462, doi:10.1063/1.1530160.

Farrell, W. M., D. A. Gurnett, and C. K. Goertz (1989), Coherent Cherenkov radiation from the Spacelab 2 electron beam, *J. Geophys. Res.*, *94*, 443–452, doi:10.1029/JA094iA01p00443.

Farrell, W. M., R. J. MacDowall, R. A. Hess, M. L. Kaiser, M. D. Desch, and R. G. Stone (1993), An interpretation of the broadband VLF waves near the Io torus as observed by Ulysses, *J. Geophys. Res.*, *98*, 21,177–21,188, doi:10.1029/93JA02591.

Gurnett, D. A. (1966), A satellite study of VLF hiss, *J. Geophys. Res.*, *71*, 5599–5615.

Gurnett, D. A., and B. J. O'Brien (1964), High-latitude geophysical studies with satellite Injun 3 5. Very low frequency electromagnetic radiation, *J. Geophys. Res.*, *69*, 65–89, doi:10.1029/JZ069i001p00065.

Gurnett, D. A., W. S. Kurth, and F. L. Scarf (1979), Auroral hiss observed near the Io plasma torus, *Nature*, *280*, 767–770, doi:10.1038/280767a0.

Gurnett, D. A., W. S. Kurth, J. T. Steinberg, P. M. Banks, R. I. Bush, and W. J. Raitt (1986), Whistler-mode radiation from the Spacelab 2 electron beam, *Geophys. Res. Lett.*, *13*, 225–228, doi:10.1029/GL013i003p00225.

Gurnett, D. A., et al. (2004), The Cassini radio and plasma wave investigation, *Space Sci. Rev.*, *114*, 395–463, doi:10.1007/s11214-004-1434-0.

Gurnett, D. A., et al. (2005), Radio and plasma wave observations at Saturn from Cassini's approach and first orbit, *Science*, *307*, 1255–1259, doi:10.1126/science.1105356.

Gurnett, D. A., A. M. Persoon, J. B. Groene, A. J. Kopf, G. B. Hospodarsky, and W. S. Kurth (2009), A north-south difference in the rotation rate of auroral hiss at Saturn: Comparison to Saturn's kilometric radio emission, *Geophys. Res. Lett.*, *36*, L21108, doi:10.1029/2009GL040774.

James, H. G. (1976), VLF saucers, *J. Geophys. Res.*, *81*, 501–514, doi:10.1029/JA081i004p00501.

Jørgensen, T. S. (1968), Interpretation of auroral hiss measured on OGO-2 and at Byrd Station in terms of incoherent Cherenkov radiation, *J. Geophys. Res.*, *73*, 1055–1069, doi:10.1029/JA073i003p01055.

Kennel, C. (1966), Low-frequency whistler mode, *Phys. Fluids*, *9*(11), 2190–2202, doi:10.1063/1.1761588.

Lönnqvist, H., M. André, L. Matson, A. Bahnsen, L. G. Blomberg, and R. E. Erlandson (1993), Generation of VLF saucer emissions observed by the Viking satellite, *J. Geophys. Res.*, *98*, 13,565–13,574, doi:10.1029/93JA00639.

Maggs, J. E. (1976), Coherent generation of VLF hiss, *J. Geophys. Res.*, *81*(10), 1707–1724, doi:10.1029/JA081i010p01707.

Martin, L. H., R. A. Helliwell, and K. R. Marks (1960), Association between aurorae and very low-frequency hiss observed at Byrd Station, Antarctica, *Nature*, *187*(4739), 751–753, doi:10.1038/187751a0.

Mitchell, D. G., et al. (2009), Ion conics and electron beams associated with auroral processes on Saturn, *J. Geophys. Res.*, *114*, A02212, doi:10.1029/2008JA013621.

Monson, S. J., P. J. Kellogg, and D. G. Cartwright (1976), Whistler mode plasma waves observed on Electron Echo 2, *J. Geophys. Res.*, *81*(13), 2193–2199, doi:10.1029/JA081i013p02193.

Morgan, D. D., D. A. Gurnett, J. D. Menietti, J. D. Winningham, and J. L. Burch (1994), Landau damping of auroral hiss, *J. Geophys. Res.*, *99*, 2471–2488, doi:10.1029/93JA02545.

Mosier, S. R., and D. A. Gurnett (1969), VLF measurements of the Poynting flux along the magnetic field with the Injun 5 satellite, *J. Geophys. Res.*, *74*, 5675–5687, doi:10.1029/JA074i024p05675.

Pfaff, R., C. Carlson, J. Watzin, D. Everett, and T. Gruner (2001), An overview of the Fast Auroral SnapshoT (FAST) satellite, *Space Sci. Rev.*, *98*, 1–32, doi:10.1023/A:1013187826070.

Rönnmark, K. (1982), WHAMP: Waves in homogenous, anisotropic multicomponent plasma, *KGI Rep. 179*, Kiruna Geophys. Inst., Kiruna, Sweden.

Rönnmark, K. (1983), Computation of the dielectric tensor of a Maxwellian plasma, *Plasma Phys.*, *25*, 699–701, doi:10.1088/0032-1028/25/6/007.

Smith, R. L. (1969), VLF observations of auroral beams as sources of a class of emission, *Nature*, *224*(5217), 351–352, doi:10.1038/224351a0.

Stix, T. H. (1962), *The Theory of Plasma Waves*, McGraw-Hill, New York.

Taylor, W. W. L., and S. D. Shawhan (1974), A test of incoherent Cherenkov radiation for VLF hiss and other magnetospheric emissions, *J. Geophys. Res.*, *79*, 105–117, doi:10.1029/JA079i001p00105.

Young, D. T., et al. (2004), Cassini plasma spectrometer investigation, *Space Sci. Rev.*, *114*, 1–112, doi:10.1007/s11214-004-1406-4.

N. André and S. Grimald, Centre d'Etude Spatiale des Rayonnements, Université Paul Sabatier, CNRS, F-31028 Toulouse, France.

C. S. Arridge and A. J. Coates, Mullard Space Science Laboratory, University College, London, Dorking, Surrey, RH5 6NT, U.K.

M. K. Dougherty, Blackett Laboratory, Imperial College, London, U.K.

D. A. Gurnett, G. B. Hospodarsky, A. J. Kopf, W. S. Kurth, J. D. Menietti, and P. Schippers, Department of Physics and Astronomy, University of Iowa, Iowa City, IA 52242, USA. (andrew-kopf@uiowa.edu)